Nanocrystalline copper oxide thin films deposited by SILAR technique: Morphological, structural, optical and antibacterial studies

K. Dhanabalan [a,*], A.Vasuhi [b], G. Padma Priya[c], A.T. Ravichandran [d],

K. Ravichandran [e], P.Karthick [f], S. Valanarasu [g],

[a] *Department of physics, J.J. College of Arts and Science (Autonomous), Pudukkottai, Tamil Nadu, India*

[b] *PG and Research Department of Physics, H.H. The Rajah's College (Autonomous), Pudukkottai, Tamil Nadu, India*

[c] *Department of Chemistry, Bharath Institute of Higher Education and Research, Bharath University, Chennai – 600 073, Tamil Nadu, India*

[d] *PG and Research Department of Physics, National College (Autonomous), Tiruchirappalli, Tamil Nadu, India*

[e] *Post Graduate and Research Department of Physics, AVVM Sri Pushpam College (Autonomous), Poondi, Thanjavur, India*

[f] *Department of Ocean Studies and Marine Biology, Pondicherry University, Port Blair, Andaman, India*

[g] *Post Graduate and Research Department of Physics, Arul Anandar College, Karumathur,*

Corresponding author E-mail: vasuhidhanabalan@gmail.com* *(K. Dhanabalan)***

ABSTRACT

Nanocrystalline copper oxide thin films were deposited onto glass substrates employing successive ionic layer adsorption and reaction (SILAR) technique. The surface morphological, microstructural, optical and antibacterial properties were studied. The structural studies revealed that as-deposited and annealed at 250°C films belong to the cubic Cu_2O phase with preferential orientation along (111) direction [JCPDS card No: 78-2076]. The antimicrobial assay was tested against Staphylococcus aureus. Nanoparticles are in demand for the usage of medical industries to control pathogens. Results obtained from Cu_2O nano-thin films possessing significant antimicrobial activity against the tested human pathogen at a maximum inhibition zone of 16 mm. The surface morphological studies showed that the needle-shaped grains play the crucial role in the antibacterial activity of the Cu_2O films. From EDAX, the presence of elements Cu and O in the product was confirmed. Atomic force microscope study depicts that the surface of the film has closely packed nearly uniform sized grains. From the TEM, the film is well oriented after annealing.

Keywords: Cu_2O, Thin Films, SILAR technique, Antibacterial activity, Scanning Electron Microscope (SEM)

1. Introduction

The advancement of nanotechnology has encouraged the researchers to explore the properties of nanoparticles (NPs) for various applications. Inorganic NPs are widely used as antimicrobial agents as they have improved safety and stability compared with organic antimicrobial agents [1]. Recently, a considerable amount of research works have been published on the anti-microbial activities of inorganic NPs. They have investigated

intensively on the potential antimicrobial activities of inorganic NPs against target bacterial and fungal pathogens [2].

The inorganic NPs are very efficient in removal of pathogens in water [3], and also they are very effective in imparting of antibacterial effect to fabric [4,5]. Metal oxide NPs have also been considered for research on catalytic and antimicrobial activities [6]. Among the various metal oxides, the copper oxide has attracted particular attention for antimicrobial activities considering its easy synthesis and useful physical properties [7, 8].

Copper oxide NPs are widely being used in many industrial applications [8]. Cotton fibers treated with copper oxide have shown significant activity against several pathogens [9, 10], the fibers possess a broad spectrum of antibacterial, antifungal, antiviral properties [10], they have strong antimicrobial activity against both Gram-positive and negative bacteria [11-14]. Increased concentration of copper oxide NPs have shown the decreased percentage of bacterial growth; particularly this effect is more in Gram-positive bacterial colonies than Gram-negative.

Generally, the nanomaterials possess more activity in the drop-test method when used with an increased concentration of NPs. In this present investigation, the antimicrobial properties of copper oxide nanocrystalline thin films prepared by SILAR technique have been analyzed.

2. Experimental Details

SILAR technique was used to prepare nanocrystalline copper oxide thin films onto glass substrates. The chemicals used in the work, copper sulfate pentahydrate ($CuSO_4.5H_2O$), Sodium thiosulfate ($Na_2S_2O_3.5H_2O$) and sodium hydroxide (NaOH) were purchased from Merck. Two separate solutions were prepared, 1.0 M of NaOH was taken in a separate glass beaker and it was kept at a temperature 85°C. At the same time, another complex solution of

copper thiosulfate was prepared by adding 0.1 M sodium thiosulfate with 0.1 M copper sulfate pentahydrate and it was stirred until a colorless solution was obtained.

The formation of colorless solution could be represented by equ (1)

$$2Cu^{2+} + 4S_2O^{3-}{}_2 \longleftrightarrow 2[Cu(S_2O_3)]^- + [S_4O_6]^{2-} \quad (1)$$

For the deposition of the film the substrate was dipped first in hot NaOH solution and cationic precursor solution (copper thiosulphate) for 30 s by holding the substrate vertically using a sample holder. Finally, it was immersed in double distilled water in order to remove the loosely bounded particles from the substrate. As a result of immersion in NaOH solution, OH^- ions from NaOH solution adhered to the substrate surface.

When the OH^- ions adhered substrate is dipped in the Cu(I) ions solution, the Cu(I) ions react with (OH^-) ions present on the surface and forms copper oxide by the reaction denoted in equ (2)

$$2Cu^+ + 2OH^- \longrightarrow Cu_2O + H_2O \quad (2)$$

This cycle of immersion in both the liquids is repeated for 2 to 3 cycles in order to get smooth and nearly transparent thin layer of Cu_2O. The number of immersion cycles required (50) was decided by inspecting the film physically. After deposition, the films were annealed at a temperature 250 °C for one hour in an air medium, and then the films were characterized by morphological, structural, optical and antibacterial properties.

SILAR deposited for as and annealed films were subjected to XRD, SEM and optical absorption studies in order to analyze the structural, morphological and optical properties respectively. X-ray diffraction pattern of the copper oxide thin film was studied using a Philips X'PETR-PRO diffractometer employing Cu Kα radiation (λ = 1.54060 Å) operated at 40 kV and 30 mA in the wide angle region from 10° to 80°. Surface morphological study of the samples was done using a scanning electron microscope (Model XL30; M/s FEi, The Netherlands). To explore the optical properties of the grown copper oxide thin films UV-

visible optical absorption and transmittance spectra were obtained using UV- visible spectrophotometer (Model: Lambda 35, Make – Perkin Elmer) in the wavelength ranges from 400 to 900 nm. Photoluminescence (PL) spectra were studied using spectro-fluorometer (JobinYvon_FLUROLOG-FL3-11). The formation of copper oxide was further confirmed by FTIR Spectroscopy (Model: Spectrum RXI, Make: Perkin Elmer). The Atomic force microscope (AFM) studies were carried out using the instrument of (Veeco-di CP II). TEM images and electron diffraction patterns for the film layers were measured using the JEOL JEM 2100, 200 KV operating voltage.

The antimicrobial assay was tested against Staphylococcus aureus a Gram-positive bacterium. Staphylococcus aureus MTCC 96 Pathogenic bacterial strain was used for this current antimicrobial study. Standard Microbial techniques were followed for media preparation. Bacterial strain was inoculated into the sterilized nutrient broth and they were incubated at 37°C for 24 hrs. Mueller Hinton Agar (HIMEDIA, MUMBAI) plate was prepared and was inoculated with 18-24 hrs old bacterial broth culture with the sterile cotton swab and the plate was incubated at 37°C for 24 hrs. Antibacterial activity was determined by following standard disc diffusion technique. Suspension of Gram-positive Staphylococcus aureus MTCC 96 culture was cotton swabbed on Muller Hinton Agar (HIMEDIA, MUMBAI) Petri plates and the nanocrystalline thin film containing substrate was placed above the swabbed culture plate. Culture plate was incubated at 37°C for 24 hrs. Growth inhibition zone produced by the substrate coated with the Cu_2O nanocrystalline thin film was measured as zones of inhibition in millimeters.

3. Results and discussion

X-ray diffraction pattern of the as-deposited and annealed Cu_2O thin films are shown in Fig. 1.The XRD profile of the as-deposited film reveals that the prepared Cu_2O films are in the cubic structure according to the JCPDS card No: 78- 2076. The film annealed at 250 °C,

shows increased the peak intensity of Cu_2O phase and it shows additional peaks comparing the as-grown films. This increase of intensity in diffraction line corresponding to preferential peak (111) indicates that good crystalline quality film is obtained after annealing at 250 °C.

The crystallite sizes of the films were calculated using Scherrer's formula [15], and the results are presented in Table 1.

$$D = \frac{0.9\lambda}{\beta \cos\theta} \tag{3}$$

where λ is the wavelength of X-ray radiation (1.5406 Å for Cu-K_α), θ is the Bragg's angle and β is the full-width at half-maximum.

It can be seen from Table 1, that crystallite size has been increased from 18.0 nm to 27.2 nm by annealing at 250 ºC. This increase in crystallite size is attributed to the recrystallization and the diffusion of smaller crystallites into the larger crystallites as explained by Oswald ripening effect. According to Oswald ripening effect, smaller particles are merged into the larger ones at or above a critical temperature. Here, the diffusion is the stepwise migration of atoms from one lattice site to another lattice site. For an atom or a particle to make such a move, it must not have sufficient energy to break the bonds, but it can have some very small lattice distortion during the displacement [16]. As the annealing temperature provides the minimum level of thermal energy required to move the atoms or particles it gives diffusive motion to the particles and consequently, the size is increased. From the study of summary, the antibacterial activity has obeyed the size-dependent mechanism of the particle. The increased of antibacterial activity with an increase in the particle size (18.0 nm for as-deposited and 27.2 nm for annealed at 250 ºC). It is the reason for the improved of antibacterial activity.

Optical transmittance spectra of as-deposited and annealed Cu_2O thin films are shown in Fig. 2. The annealed film has shown decreased transmittance comparing with the as-grown

film. Energy band gap values of the grown Cu_2O thin films were obtained using the optical transmittance measurements, they were obtained by linear extrapolation of the graph of $(\alpha h\nu)^2$ versus photon energy($h\nu$) based on the Tauc`s relation [19] given below.

$$\alpha h\nu = A(h\nu - E_g)^{1/2} \quad (4)$$

where α is absorption coefficient, A is a constant, E_g is the optical band gap.

From the results, the band gap value of as-deposited and annealed film found to be 2.3 eV and 2.0 eV [20]. The inset of Fig (2) shows energy band gap value. The values are in good agreement with the reported optical band gap for the crystalline phase of Cu_2O thin films [21]. The decrease in band-gap for the annealed film may be due to absorption by the defect states.

Fig. 3 shows the FTIR spectrum of the as-grown and annealed Cu_2O thin films. The spectrum shows the presence of metal oxide material in the region of 400 cm^{-1} to 600 cm^{-1}. The peaks presented around 460 $cm^{-1}$and 577 cm^{-1}corresponds to stretching vibrational behavior of Cu – O of (111) and (200) planes. The strong absorption peak obtained at 610 cm^{-1}conforms that the synthesized products are is the component of Cu_2O [22]. The broad absorption bands obtained between 1300 cm^{-1} to 2000 cm^{-1} are attributed to H_2O and CO_2 molecules of the Cu_2O nanocrystalline thin films. The broad band of the spectrum nearly at 3400 cm^{-1} is attributed corresponding to the stretching vibration of OH groups and nearly at 3260 cm^{-1} represent the N-H stretching vibration. The band at 2917 cm^{-1} and 2850 cm^{-1} is attributed with respect to the asymmetric C-H and symmetric C-H stretch vibrations.

Fig.4 shows the room temperature photoluminescence (PL) spectrum obtained for the as-deposited and annealedCu_2O thin films. PL emission of materials is the result of the electron-hole separation or recombination from the electron-photon scattering process. After annealing at 250 ºC the intensity of the spectrum is improved. It is evident that the crystallinity of the film is improved due to annealing. The broadened peak obtained for the

as-grown film may be attributed to the small grain size of the Cu_2O thin film. The PL spectrum obtained has exhibited UV and visible emission of the peak at 372, 431 (blue region), 450 (blue region) and 543 (Green region). The different emission of peaks may be attributed to the variation modes of crystalline Cu_2O particles.

Surface morphology of the prepared Cu_2O thin film for as-deposited and annealed at 250 ºC film was observed by Scanning Electron Microscope (SEM). SEM image of the film grown using optimized condition is shown in the Fig.5. The formation of needle-shaped particles can be explained by the process of nucleation and coalescence. All the needle shaped particles are arranged uniformly with hierarchical effect. The hierarchical effective material of copper oxide is highly obeyed by the antibacterial activity [17]. Recently demonstrated Cu_2O nanoparticles are excellent action against S.aureus bacteria [18]. After annealing, the surface of the film is shown with mixed grains of needle and microsphere particles. For the as-deposited film grains of various lengths covering the entire substrate area and the length of the nanorods is found to vary between 50 to 100 nm. EDAX spectrum taken for the annealed film at 250 ° C as shown in Fig. (6). It confirms the presence of the elements Cu and O in the product.

Fig. (7) shows the TEM images of as-deposited and annealed at 250° C with corresponding images of nanoparticles and nanobelts. Fig. (7-a) the image clearly shows the non-uniformity of the grains on the surface of the film. Fig (7-b) shows the uniformity of the grains with needle-shaped has been on the surface of the film when annealed at 250 ºC. From this study, the quality of the film increased after annealing. This result is correlated with XRD and SEM.

Fig. (8) shows the AFM images of as-deposited and annealed at 250° C film. From the figure, the grain size is found to increase and the surface has heavily packed needle-

shaped grains which are the characteristic feature of Cu_2O film. The AFM images also support the above-mentioned observations.

Copper oxide thin films highly obey the antibacterial activities of gram-positive S. aureus and gram-negative E.coli. Copper is one of the most important enzymes in many living microorganisms. But, more free Cu^{2+} ions at a high concentration are able to produce hazardous effects to produce reactive oxygen species (ROS) [23]. This effect is drastically affected by secretion of the amino acid as well as DNA [24].The production of ROS by copper oxide is environmentally modified during the antibacterial test. Finally, the produced ROS is initially interacted with outer walls only and it was further generated the free radicals of inner cell membranes and the cell become disappeared. Because the electron-hole recombination is produced heat in the inside of the copper oxide thin film [25].

The nano-thin films of as-deposited and annealed at 250 ºC were screened for antimicrobial activity against the S. aureus. The nanoparticle contains annealed glass plate has shown antibacterial activity against S.aureus (16mm) and nanoparticles contain in as-deposited glass plate has shown a minimum zone of inhibition (7mm). The zone of inhibition was more in 16-18 hrs and zone of inhibition was reduced to (6mm) after 24 hrs.

Several investigations carried out earlier employing Cu_2O nanoparticles against E.coli and S. aureus revealed the considerable influence of Cu_2O nanoparticles. Recent studies revealed Cu_2O nanoparticles coated on cotton fiber show antibacterial activity against both Gram-negative E. coli and Gram-positive S.aureus bacteria [8]. Earlier Cu_2O nanoparticles were shown to be very effective against both gram-negative and gram-positive bacteria, which increases the rate of resistance to the pathogens when the concentration of nanoparticles increases [10]. Cu_2O nano fibers have been reported as exhibiting properties that enable to control the E.coli and S.aureus [26]. In this study, it has been observed that the nanocrystalline Cu_2O thin film prepared by SILAR technique can exhibit antibacterial

activity from 18 to 24 hrs of incubation time. The nanocrystalline Cu_2O films have exhibited antimicrobial activity against Gram-positive S. aureus. This study also supports the results of the earlier studies on the effect of concentration of nanoparticles. The increase of the concentration of nanoparticles will decrease the bacterial growth, this may be due to the reduction of voids providing space for the growth of bacteria and it remains resistance against the particular pathogenic bacterial strain.

4. Conclusions

Deposition of copper oxide thin films through SILAR technique was successfully demonstrated. The thin films thus grown were systematically characterized for their morphology and optical properties. The SEM characterization of the films has the shown needle-shaped Cu_2O films. The band gap of the film calculated is found to be 2.3eV to2.0 eV which is well matched with the literature of Cu_2O. This Cu_2O nanoparticle deposited on glass plates have exhibited moderate antimicrobial activity against Staphylococcus aureus. The AFM and TEM images are clearly shown, that the crystalline quality of the film is improved for the annealed film at 250 ^{o} C. Further work is underway to check the effect of the bactericidal activity of Cu_2O nanoparticles against S. aureus and other gram positive and gram negative bacterial and fungal pathogens.

Acknowledgement

Our special thanks to Dr.R. Chandramohan, Principal, Sree Sevugan Annamalai College, Devakottai, Tamilnadu, India, for his kind encouragement. The Principal author A.T. Ravichandran thanks, UGC-MRP: F.No 41-937/2012(SR), New Delhi for the partial funding of the work through a major research grant.

References

[1] P. Pandey, M. S. Packiyaraj, H. Nigam, G. S. Agarwal, B. Singh and K.P. Manoj, Antimicrobial properties of CuO nanorods and multi-armed nanoparticles against B. anthracis vegetative cells and endospores, *Beilstein J. Nanotechnol,* vol. 5, 789 **(2014).**

[2] G Padmapriya, A Manikandan, V Krishnasamy, S. K. Jaganathan, and S Arul Antony, Spinel $Ni_xZn_{1-x}Fe_2O_4$ ($0.0 \leq x \leq 1.0$) nano-photocatalysts: Synthesis, characterization and photocatalytic degradation of methylene blue dye, *J. Mol. Struct.* vol. 1119, 39-47 **(2016)**

[3] B.A. Josephine, A. Manikandan, V.M. Teresita, and S.A. Antony, Fundamental study of $LaMg_xCr_{1-x}O_{3-\delta}$ perovskites nano-photocatalysts: Sol-gel synthesis, characterization and humidity sensing, *Korean J. Chem. Eng*. vol. 33, 1590-1598 **(2016)**

[4] A. G. Abraham, A. Manikandan, E. Manikandan, S.Vadivel, S.K.Jaganathan, A. Baykal, and P. S. Renganathan, Enhanced magneto-optical and photo-catalytic properties of transition metal cobalt (Co^{2+} ions) doped spinel $MgFe_2O_4$ ferrite nanocomposites, *J. Magn. Magn. Mater*. vol. 452, 380-388 **(2018)**

[5] D Maruthamani, S Vadivel, M Kumaravel, B Saravanakumar, B. Paul, S. S. Dhar, A. H.Yangjeh, A Manikandan, and G. Ramadoss, Fine cutting edge shaped Bi_2O_3 rods/reduced graphene oxide (RGO) composite for supercapacitor and visible-light photocatalytic applications, *J. Colloid Interf. Sci.* vol. 498, 449-459 **(2017)**

[6] Z. Jia, D. Ren, Y. Liang, and R. Zhu, A new strategy for the preparation of. porous zinc ferrite nanorods with subsequently light-driven photocatalytic Activity, *Mater. Lett.* vol. 65, 3116-3119 **(2011)**

[7] Y. Zheng, C. Chen, Y. Zhan, X. Lin, Q. Zheng, K. Wei, J. Zhu, and Y. Zhu, Luminescence and photocatalytic activity of ZnO nanocrystals: Correlation between Structure and Property, *Inorg. Chem*. vol. 46, 6675-6682 **(2007)**

[8] A. K. Carlos, G. F. Wypych, G. M. Sandra, N. Duran, N. Nagata, and P. Z. Peralta, Semiconductor-assisted photocatalytic degradation of reactive dyes in aqueous solution, *Chemosphere*, vol. 40, 433-440 **(2000)**

[9] A Shameem, P Devendran, V Siva, M Raja, SA Bahadur, and A Manikandan, Preparation and Characterization Studies of Nanostructured CdO Thin Films by SILAR Method for Photocatalytic Applications, *J. Inorg. Organomet. Polym.* Vol. 27 (3), 692-699 **(2017)**

[10] A. G. Abraham, A. Manikandan, E. Manikandan, S.Vadivel, S.K.Jaganathan, A. Baykal, and P. S. Renganathan, Enhanced magneto-optical and photo-catalytic properties of transition metal cobalt (Co^{2+} ions) doped spinel $MgFe_2O_4$ ferrite nanocomposites, *J. Magn. Magn. Mater*. vol. 452, 380-388 **(2018)**

[11] C. N. Mohan, V. Renuga, and A. Manikandan, Influence of silver precursor concentration on structural, optical and morphological properties of $Cu_{1-x}Ag_xInS_2$ semiconductor nanocrystals, *J. Alloys Compd*. vol. 729, 407-417 **(2017)**

[12] D. Gao, Z. Shi, Y. Xu, J. Zhang, G. Yang, J. Zhang, X. Wang, and D. Xue, Synthesis, Magnetic Anisotropy and Optical Properties of Preferred Oriented Zinc Ferrite Nanowire Arrays, *Nanoscale Res. Lett*. vol. 5, 1289-1294 **(2010)**

[13] G. Fan, Z. Gu, L. Yang, and F. Li, Nanocrystalline zinc ferrite photocatalysts formed using the colloid mill and hydrothermal technique, *Chem. Eng. J*. vol. 155, 534-541 **(2009)**

[14] S. Joshi, and M. Kumar, Influence of Co^{2+} Substitution on Cation Distribution and on Different Properties of $NiFe_2O_4$ Nanoparticles, *J. Supercond. Nov. Magn*. vol. 29, 1561-1572 **(2016)**

[15] C. Barathiraja, A. Manikandan, A.M.U. Mohideen, S. Jayasree, and S.A. Antony, Magnetically recyclable spinel $Mn_xNi_{1-x}Fe_2O_4$ (x= 0.0–0.5) nano-photocatalysts: structural, morphological and opto-magnetic properties, *J. Supercond. Nov. Magn*. vol. 29, 477-486 **(2016)**

[16] A. Silambarasu, A. Manikandan, K Balakrishnan, S. K. Jaganathan, E. Manikandan, and J. S. Aanand, Comparative Study of Structural, Morphological, Magneto-Optical and Photo-Catalytic Properties of Magnetically Reusable Spinel $MnFe_2O_4$ Nano-Catalysts, *J. Nanosci. Nanotech.* vol. 18, 3523-3531 **(2018)**

[17] M. Aliahmad, and M.Noori, Synthesis and characterization of nickel ferrite nanoparticles by chemical method, Indian J. Phys. vol. 87, 431-434 **(2013)**

[18] A.M.Banerjee, M.R. Pai, S.S. Meena, AK. Tripathi, and S.R. Bharadwaj, Catalytic activities of cobalt, nickel and copper ferrospinels for sulfuric acid decomposition: The high temperature step in the sulfur based thermochemical water splitting cycles, Int. J. Hydrogen Energ. vol. 36, 4768-4780 **(2011)**

[19] V Umapathy, A Manikandan, P Ramu, S Arul Antony, and P Neeraja, Synthesis and characterization of $Fe_2(MoO_4)_3$ nano-photocatalyst by simple sol–gel method, J. Nanosci. Nanotech. vol. 16, 987-993 **(2016)**

[20] K. Seevakan, A. Manikandan, P. Devendran, A. Shameem, T. Alagesan, Microwave combustion synthesis, magneto-optical and electrochemical properties of $NiMoO_4$ nanoparticles for supercapacitor application, *Ceramics International*, 44, 13879-13887 **(2018).**

[21] K. Seevakan, A. Manikandan, P. Devendran, A. Baykal, T. Alagesan, Electrochemical and magento-optical properties of cobalt molybdate nano-catalysts as high-performance supercapacitors, *Ceramics International*, 44, 17735-17742 **(2018).**

[22] R. Bomila, S. Srinivasan, S. Gunasekaran, A. Manikandan, Enhanced photocatalytic degradation of methylene blue dye, opto-magnetic and antibacterial behaviour of pure and La-doped ZnO nanoparticles, *Journal of Superconductivity and Novel Magnetism*, 31, 855–864 **(2018).**

[23] A. T. Ravichandran, J. Srinivas, R. Karthick, A. Manikandan, A. Baykal, Facile combustion synthesis, structural, morphological, optical and antibacterial studies of $Bi_{1-x}Al_xFeO_3$ ($0.0 \leq x \leq 0.15$) nanoparticles, *Ceramics International*, 44, 13247-13252 **(2018).**

[24] K. Chitra, K. Reena, A. Manikandan, S. Arul Antony, Antibacterial studies and effect of poloxamer on gold nanoparticles by *Zingiber officinale* extracted green synthesis, *Journal of Nanoscience and Nanotechnology*, 15, 4984-4991 **(2015).**

[25] K. Chitra, A. Manikandan, S. Moortheswaran, K. Reena, S. Arul Antony, *Zingiber officinale* extracted green synthesis of copper nanoparticles: Structural, morphological and antibacterial studies, *Advanced Science, Engineering and Medicine*, 7, 710-716 **(2015).**

[26] A. Manikandan, E. Manikandan, B. Meenatchi, S. Vadivel, S. K. Jaganathan, R. Ladchumananandasivam, M. Henini, M. Maaza, Jagathrakshakan Sundeep Aanand, Rare earth element Lanthanum doped zinc oxide (La: ZnO) nanoparticles: Synthesis structural optical and antibacterial studies, *Journal of Alloys and Compounds* 723, 1155-1161 **(2017).**

Figure Captions

Fig. 1. XRD patterns of Cu_2O thin films for as-deposited and annealed at 250°C/ 1 hr.

Fig: 2. Transmittance spectrum of as-deposited and annealed Copper oxide thin films.

Fig. 3. FTIR Spectra of Cu_2O thin films for as deposited and annealed at 250° C.

Fig: 4. PL Spectra of Cu_2O thin films for as-deposited and annealed at 250° C.

Fig. 5. SEM images of Copper oxide thin films for (a) as-deposited and (b) annealed at 250° C.

Fig. 6. EDAX Spectrum of Cu_2O thin films with annealed at 250° C.

Fig. 7. TEM images of Cu_2O thin films for (a) as-deposited and (b) annealed at 250° C [image shows nanoparticles and nanobelts respectively]

Fig. 8. AFM images of (a). as deposited and (b). annealed Cu_2O films

Figures

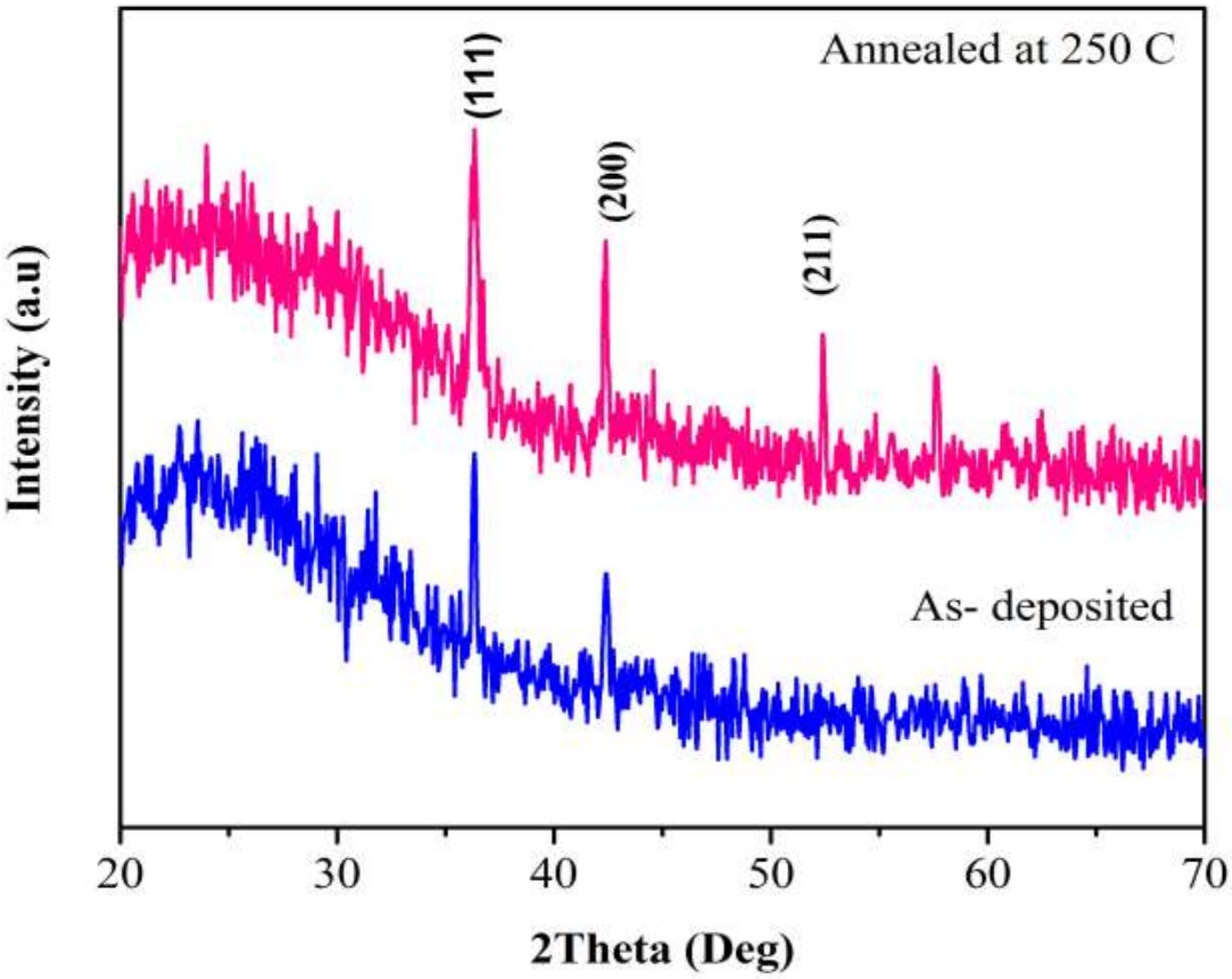

Fig. 1.

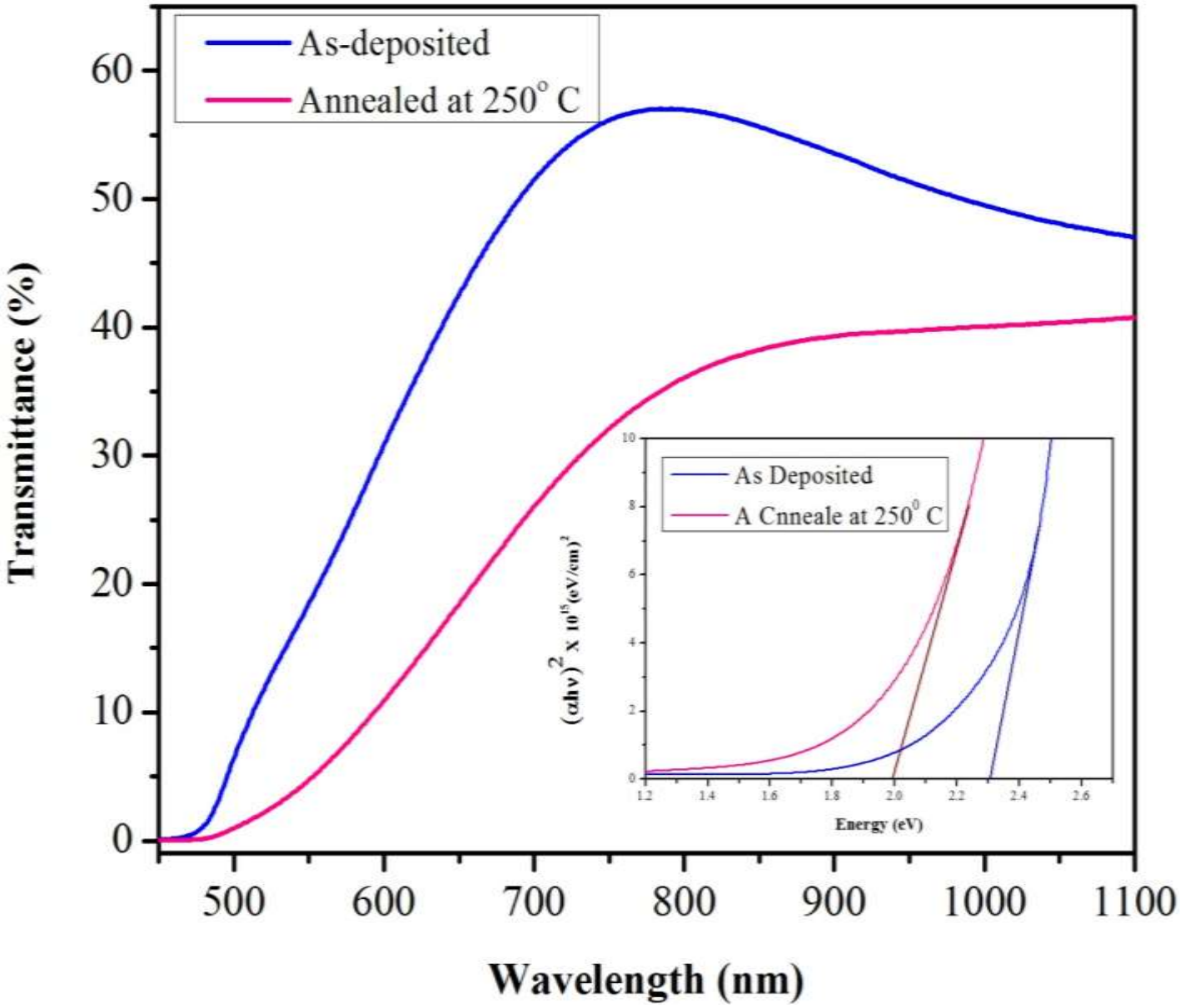
As-deposited
Annealed at 250° C
Transmittance (%)
Wavelength (nm)
0
10
20
30
40
50
60
500
600
700
800
900
1000
1100
As Deposited
A Cnneale at 250° C
(αhν)² X 10¹⁵(eV/cm)²
Energy (eV)
0
2
4
6
8
10
1.2
1.4
1.6
1.8
2.0
2.2
2.4
2.6

Fig. 2.

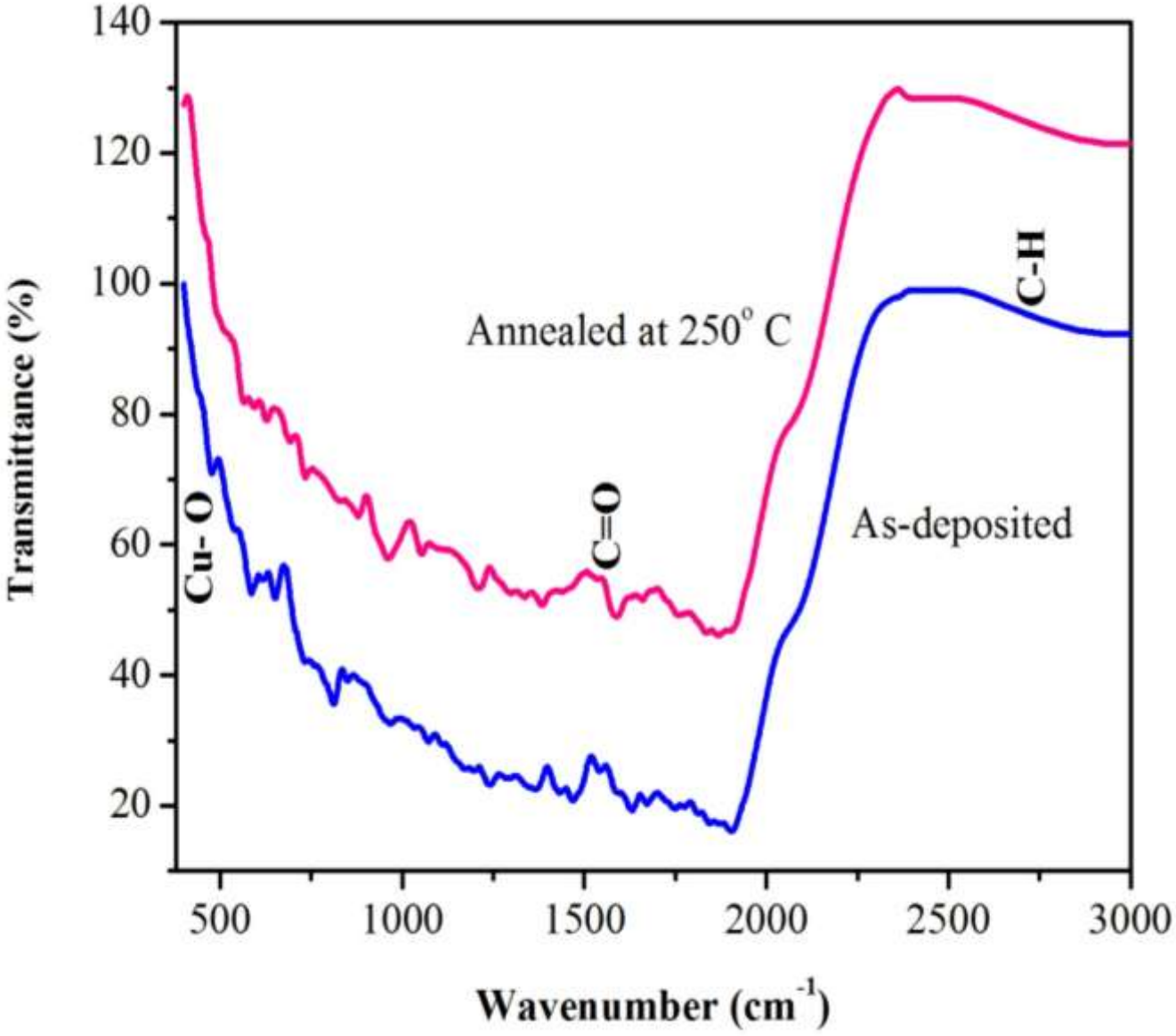
Transmittance (%)
140
120
100
80
60
40
20
500
1000
1500
2000
2500
3000
Wavenumber (cm-1)
Annealed at 250° C
As-deposited
Cu- O
C=O
C-H

Fig. 3.

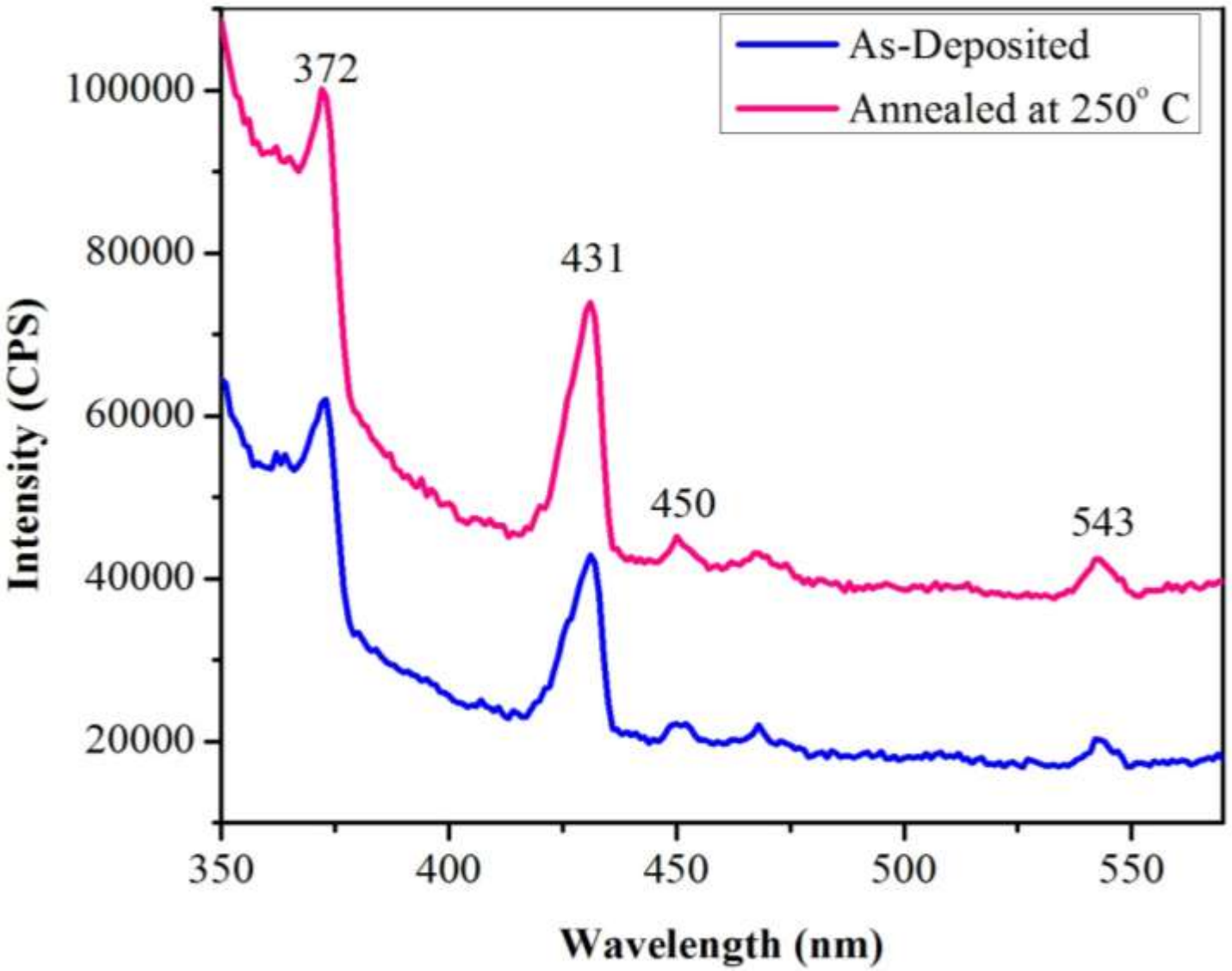
As-Deposited
Annealed at 250° C
372
431
450
543
100000
80000
60000
40000
20000
Intensity (CPS)
350
400
450
500
550
Wavelength (nm)

Fig: 4.

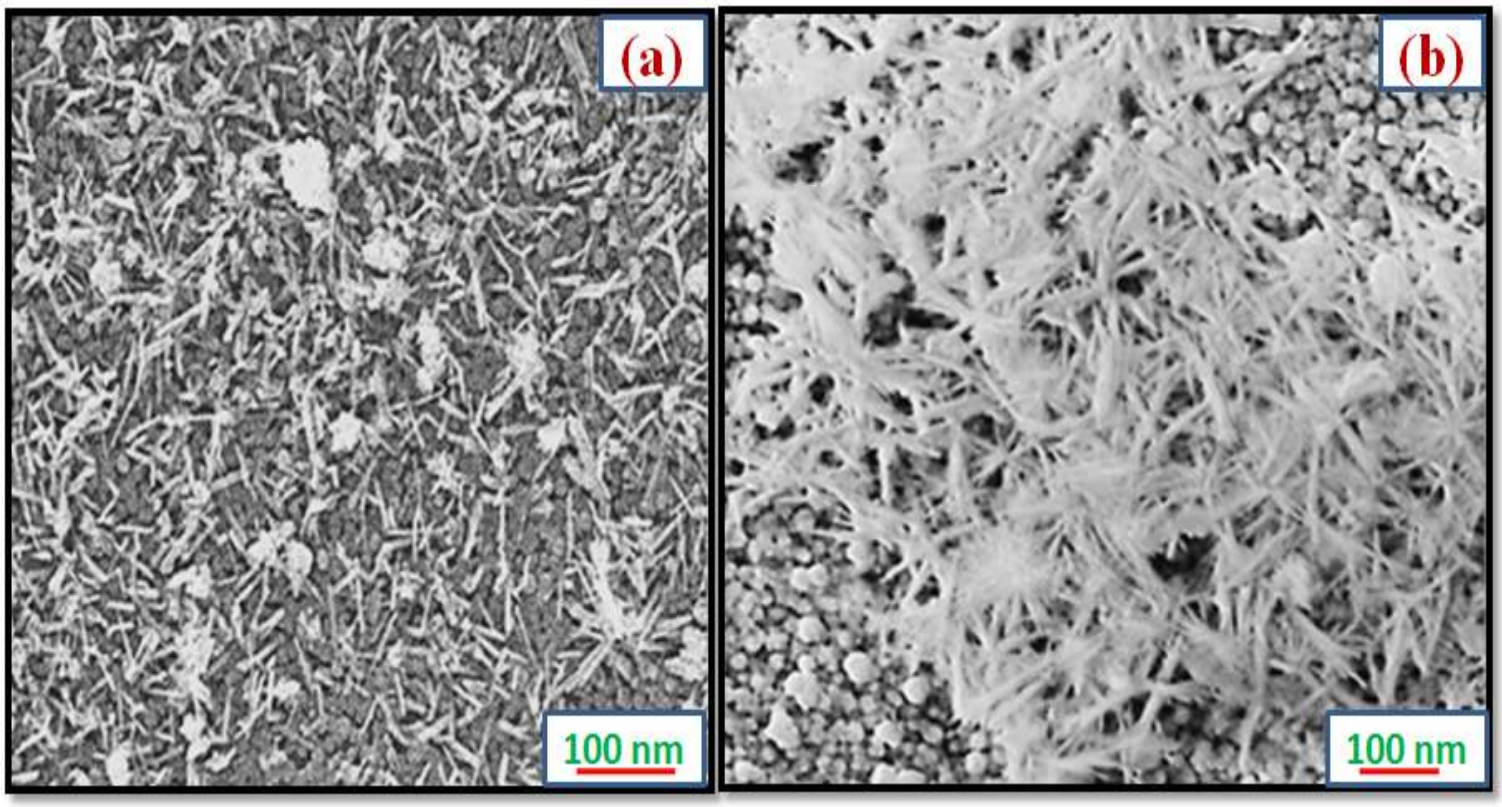

Fig. 5.

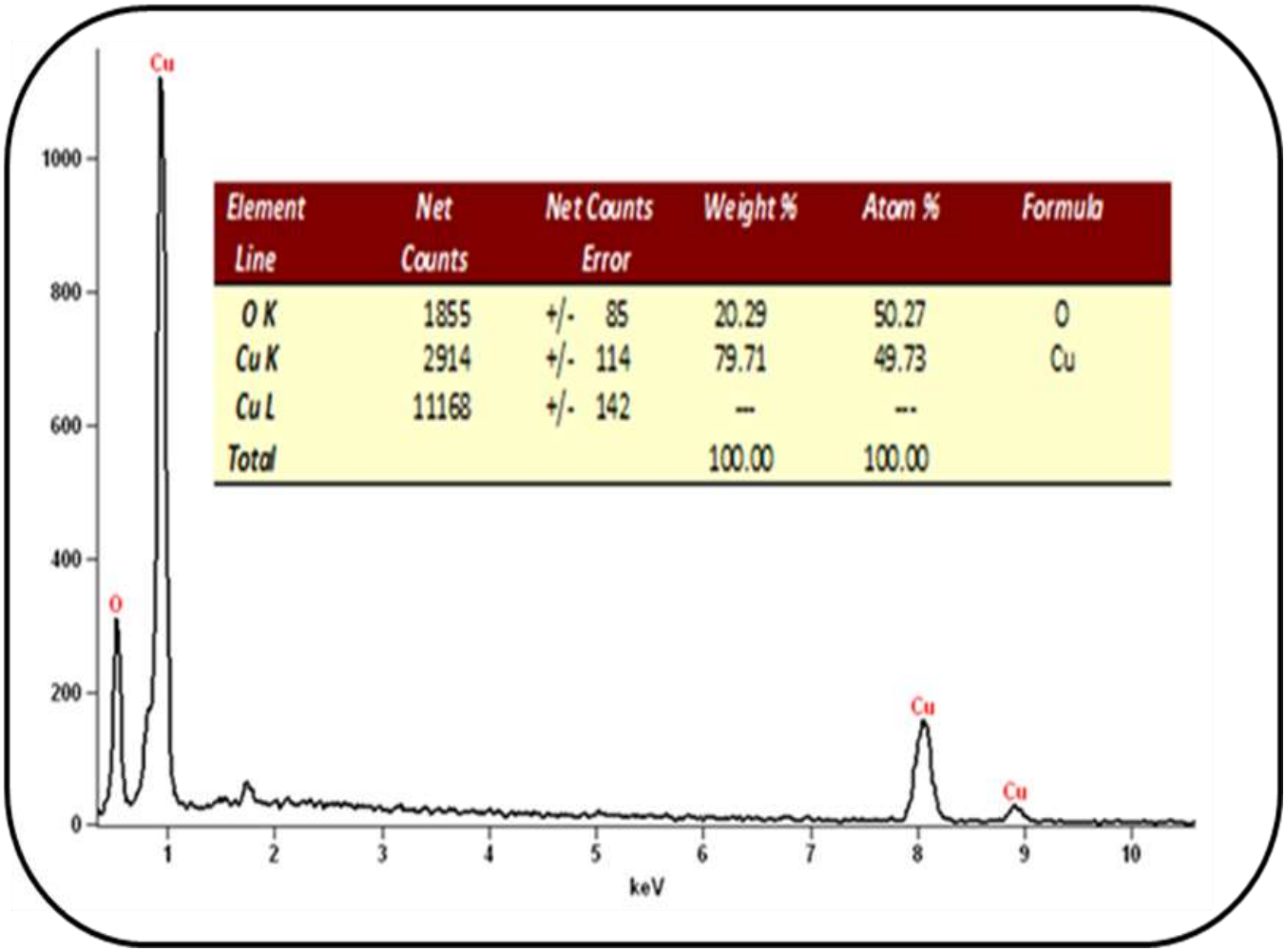

Element Line	Net Counts	Net Counts Error	Weight %	Atom %	Formula
O K	1855	+/- 85	20.29	50.27	O
Cu K	2914	+/- 114	79.71	49.73	Cu
Cu L	11168	+/- 142	---	---	
Total			100.00	100.00	

Fig. 6.

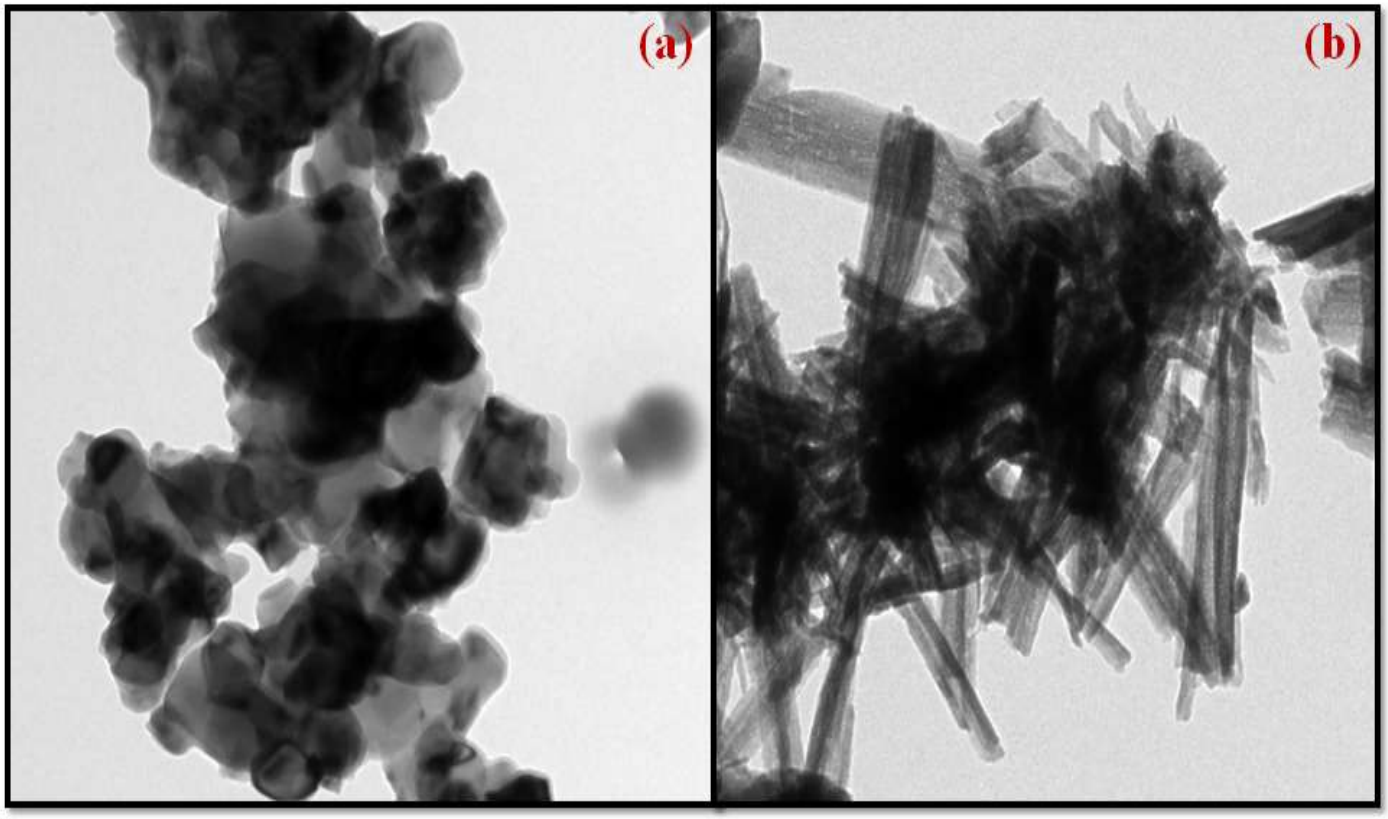

Fig. 7.

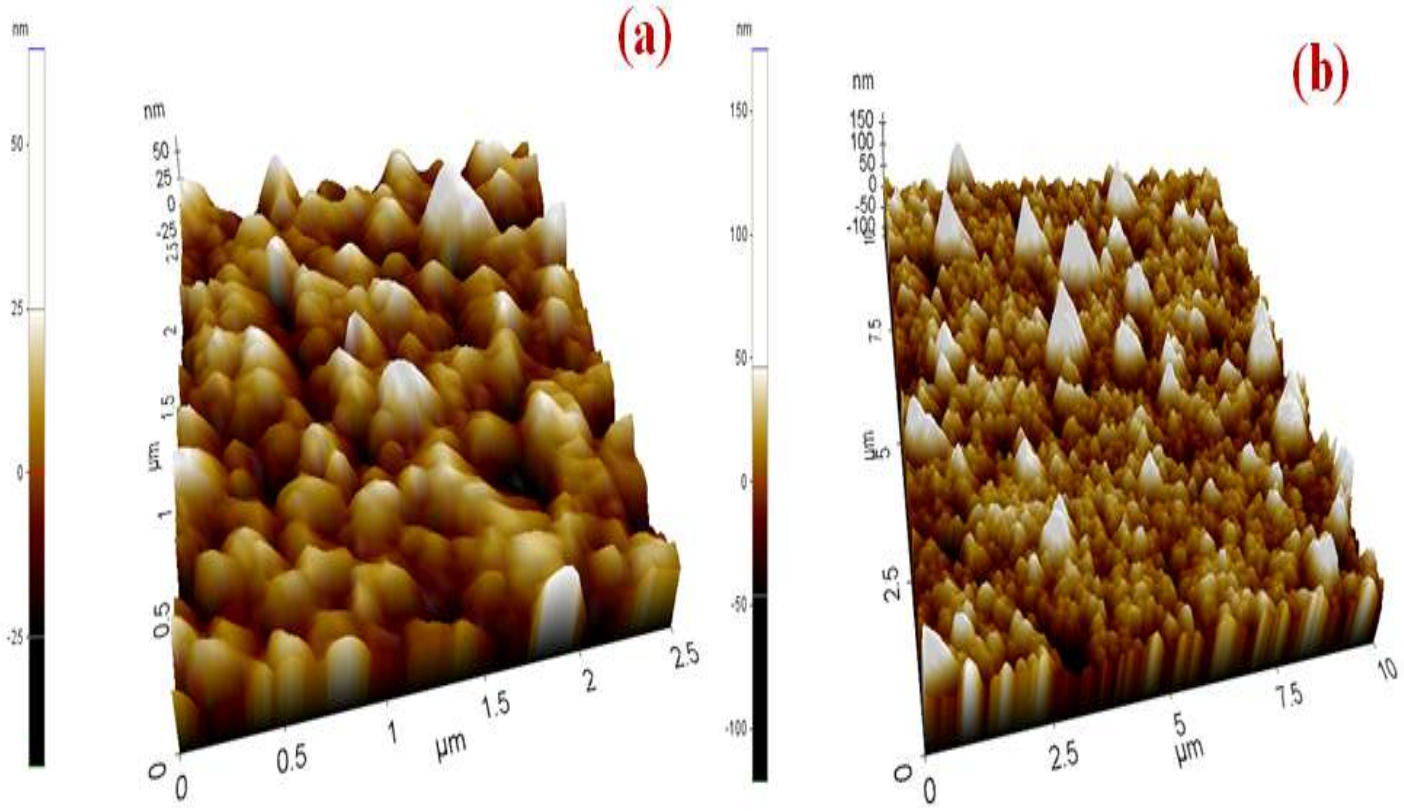
(a)
nm
50
25
0
-25
nm
50
25
0
-25
2
1.5
1
0.5
0
µm
0
0.5
1
1.5
2
2.5
nm
150
100
50
0
-50
-100
(b)
nm
150
100
50
0
-50
-100
7.5
5
2.5
0
µm
0
2.5
5
7.5
10

Fig. 8.

Table 1. Structural and optical parameters of as-deposited and annealed Cu_2O thin films

Samples		XRD Analysis			JCPDS Card	Energy band gap E_g(eV)	Grain size (nm)
S.No	Temp °C	Phase	hkl	2θ(°)			
1.	As-Deposited	Cu_2O	111	36.32	78- 2076	2.3	18.0
2.	Annealed 250°C	Cu_2O	111	36.27	78- 2076	2.0	27.2